Webology (ISSN: 1735-188X)
Volume 18, Number 6, 2021

A Reversible Watermarking Model To Autheticate Medical Images Using Optimum Linear Filtering

Veena s[1] , Dr. C K Narayanappa[2] , Dr. Shivaprakash G[3]

[1]Research scholar, MED, MRSIT.

[2]Asst. Prof MSRIT (MED).

[3]Asst Prof MSRIT(EIE).

Abstract: Recently, a major enhancement in utilization of internet based services worldwide have given rise to online medical facilities where patients can interact with doctors and medical experts and can share their details via different online platforms and applications. On the other side, medical experts too share medical details like their CT scan images, X-rays, fundus images, MRI images as well as other private and confidential information with other experts or patients on online platforms which is at risk in terms of security. Any intruder or mischief can temper these information and create problems. Thus, data authenticity and data recovery while tempering occurs are two major issues which need to be discussed. Therefore, a Reversible Watermarking Technique is presented to authenticate medical images like CT scan images, X-rays, fundus images, MRI images and to localize tempering region and to retrieve tempered region. Here, these objectives are achieved using Optimum linear filtering method which optimizes two NP-hard problems like Information Loss Minimization (ILM) Problem and Reversible Watermarking Capacity Enhancement (RWCE) Problem for Reduction of Error Estimation (REE) to enhance performance efficiency. Experimental results are carried out considering different medical images under various attacks and compared with several state-of-art-watermarking schemes in terms of PSNR, SSIM, BER and NCC.

Keywords: Reversible Watermarking, Optimum linear filtering, Reduction of Error Estimation (REE), Information Loss Minimization (ILM) Problem and Reversible Watermarking Capacity Enhancement (RWCE) Problem

1 Introduction:

Recently, the utilization of image analysis techniques and image processing have drastically enhanced, especially in case of medical applications. This techniques and diagnosis methods are immensely popular in healthcare research with the objective of providing highly efficient and faster medical facilities which can sort out medical problems conveniently [1]. Moreover, in near future, telemedicine applications can become a significant method to deliver medical facilities to the patients conveniently [2]. However, the speedy growth of several technologies in recent time such as 5G technologies, cloud storage methods, big data and cloud computing applications have affected traditional way of living to a great extent. Specifically, after the emergence of Internet of Medical Things (IoMT), there are several new diagnosis techniques and treatment methods like telemedicine applications, hierarchical diagnosis methods, internet medicine applications, online consultations and intelligent medicine have continuously emerged. However, due to emergence of these advanced diagnosis methods and treatment modes and utilization of simulated surgeries, online consultations and virtual reality for medical applications have enable doctors and medical experts to share patient's private information like MRI, CT scan, Ultrasound images over online platform. Many telemedicine applications share such as auxiliary medical equipment and documents as well for better diagnosis and effective analysis. Even, they access remote image centers and hospital image clouds, communication and image arching systems for online remote consultation and cloud reading [3]. For an instance, in tele radiology applications, doctors and medical experts share CT scan images of patients to the other medical experts or radiologists over publicly available internet network for clinical diagnosis.

However, these kind of patient data and image transmission can be dangerous and prove costly due to hacking, tempering and fraudulent until unless there is a certain protection layer to keep patient data safe. Patient data tampering can cause miscommunication and misdiagnosis [4]. Several legal and ethical problems can arise due to medical data tempering like image fraud and retention, illegal data handling and privacy issues. In 1993, a standard security measure is set by Digital Imaging and Communications in Medicine (DICOM) for the effective and protective communication as well as to handle medical image information. However, advance safety guidelines and security measures of medical data and records are not effective yet according to the modern requirements [5]. Due to this digitalized medical image data like computerized tomography (CT) scan images, X-rays, fundus images, MRI images can tempered and forged without any difficulty by the intruders. Therefore, it become necessary to authenticate medical image owners before diagnosis and sharing of medical data for clinical diagnosis to other experts over an internet platform. However, regulation and guidelines on the medical images' integrity is crucial. Thus, privacy and security has become critical issue for healthcare images.

Therefore, to sort out above mentioned issues, several digital signature approaches are introduced for image and medical data authentication which works upon cryptographic algorithms [6]. However, these methods are to recognize whether medical data or image is tempered or not.

Even, these methods cannot locate the exact region in the attacked image. Therefore, watermarking methods can be the best choice for image authentication where owners of medical images can share images or medical data after image authentication. These methods are efficient enough to perform several tasks like authentication of medical images, image tempering recognition, identification of tempering region and even able to recover tempered regions [7-8]. Generally, watermarking techniques are segregated into two parts where first one is reversible watermarking techniques and the second one is irreversible watermarking techniques. In reversible watermarking, recovery of tempered region is possible from host images without any data loss and it can be recovered as original image [9]. However, in irreversible watermarking, such facilities are not present [10]. Therefore, many experts have suggested utilization of reversible watermarking techniques [11].

Several researchers have shown immense interest for the utilization of watermarking methods to authenticate medical images. Some of the literature work has been discussed below regarding watermarking of medical images. In [12], a reversible watermarking method is adopted based on the extraction of Region of Interest (ROI) to authenticate CT scan images. Here, adopted watermarking method perform content authentication as well as copyright protection. This method reduces overhead while location map generation and ROI selection. In [13], a robust reversible watermarking method is introduced for the protection of medical images and maintain integrity with the help of image authentication. Here, recursive dither modulation (RDM) is employed to eliminate biases while diagnosis. Image authenticity is obtained by combining RDM with Slant-let transform. In [14], a fragile watermarking scheme is generated for the effective authentication of medical images and recognition of tempered location in attacked image. Here, fragile watermarking methods self-recovered lost information with high accuracy based on two-hierarchical restoration method. In [15], a robust watermarking method is employed to authenticate medical data based on 3D hyperchaos and 3D dual-tree complex wavelet transform. Here, Zero embedding and blind extraction methods are also employed for the conversion of medical data into diagnosis form.

However, these watermarking methods works with spatial domain of ROI. Thus, simple embedded watermarking methods does not perform well in case of attack on medical images which can cause failure in recovery of information from tempered images. Therefore, in this article, a Reversible Watermarking Technique is employed to authenticate medical images like CT scan images, X-rays, fundus images, MRI images. Here, the proposed reversible watermarking technique minimizes optimizes two problems such as Information Loss Minimization (ILM) Problem and Reversible Watermarking Capacity Enhancement (RWCE) Problem for Reduction of Error Estimation (REE) to determine high efficiency results for authentication of medical images. Furthermore, proposed reversible watermarking technique also determine the nature of these problem and nature of their respective decision model. Here, Optimum linear filtering algorithms are utilized to optimize these problems as well as enhance efficiency of performance parameters of proposed watermarking techniques. Moreover, automatic regressive approach along

with optimum linear filtering algorithm provides effective lossless compression. Experimental results verifies superiority of proposed reversible watermarking technique compare to several watermarking schemes considering different performance metrics.

This paper is presented in the following manner. Section 2, describes about the related work presented regarding authentication of medical images though watermarking schemes and their implementation issues and how those issues can be handle with the help of the proposed reversible watermarking technique. Section 3, discusses about the methodology proposed for the efficient implementation of reversible watermarking technique to increase performance efficiency. Section 4 discusses about the simulation results and their comparison with traditional watermarking schemes and section 5 concludes the paper.

2 Related Work:

Recently, e-medical applications have attracted a lot of attention by whole research community across the world and due to availability of novel commination techniques, these applications can provide several important medical services. However, in current generation, significance of protection and authentication for digitalized medical data or images is immense. Several radiologists share patient's private medical information in form of multimedia data, such as images, audio recordings, video files which require to be protected before sharing. However, watermarking methods are capable of providing facilities like medical image authentication, tempered image identification and detection of tempered region and recovery of those region as pristine image. Thus, research community has shown great interest in developing watermarking techniques for practical implementation in real-time. Some of the literatures are presented in below paragraph related to watermarking techniques.

In [16], a review article is presented based on Digital Steganography and Watermarking schemes for authentication of medical images. In this article, several papers are reviewed regrading data hiding in digitalized medical images. This article efficiently identify problems arises in Digital Steganography and Watermarking schemes. In [17], a reversible Electronic Health Records (EHR) architecture is employed based on high payload for security and authentication of Internet of Medical Things (IoMT). Here, authentication is achieved based on Left Data Mapping (LDM), encryption methods and Pixel Repetition Method (PRM). Here, temper detection and localization is also achieved. In [18], a medical image watermarking algorithm is employed for authentication of Retinal images. Here, fast curvelet transform (FCT) methods are adopted for accurate recovery of tempered regions in attacked images. In [19], a dynamic Image Steganography technique is introduced for medical and healthcare data authentication. Along with that Image Region Decomposition (IRD) algorithm is adopted for the performance metric efficiency enhancement of MRI images. In [20], a review article is presented for reversible watermarking and data hiding. This method is utilized to obtain hidden secret messages without any Bias. In this technique, transmission of data is protected with high security level. In [21], a reversible image authentication algorithm is presented based on the secret sharing method to improve medical image sharing

efficiency. Binarization operation is performed for data recovery from tempered image. In [22], a novel information hiding evaluation method is employed for medical image authentication. This technique analyses and evaluates parameters to select highly efficient watermarking and stenography algorithms. Pneumonia Chest Xray dataset is utilized for performance testing. In [23], a deep neural network based lose less watermarking algorithm is introduced for medical image authentication and data recovery. Watermarking is conducted based on the ROI of medical images. Here, three fully connected layers are used for detection of distorted regions.

However, very few techniques have minimized optimization problems to enhance performance efficiency in Bias identification which is a quite challenging and complex process. And authentication of medical images through watermarking have many challenges such as minimization of optimization problem, performance metric efficiency enhancement and image compression, leakage of confidential information, copyright protection on medical images. Therefore, reversible watermarking technique is presented for the authentication of medical images and to improve performance efficiency.

3 Modelling for Reversible Watermarking Technique:

This section discusses about the mathematical modelling of proposed reversible watermarking technique for the authentication of medical images like CT scan image, MRI images and fundus images. Here, a detailed mathematical modelling for the optimization of Information Loss Minimization (ILM) Problem and Reversible Watermarking Capacity Enhancement (RWCE) Problem for Reduction of Error Estimation (REE) is presented which is used for the performance efficiency improvement. Here, mathematical modelling regrading embedding and removal procedure of Reduction of Error Estimation (REE) using reversible watermarking technique is demonstrated in below section for performance metric efficiency enhancement in medical imaging.

3.1 Embedded method of Reduction of Error Estimation (REE):

First of all, determine the image resolution (pixel information) from cover image using image pixel estimation function. All the pixels have a steering relationship between each other. Assume that group of cover image pixels is expressed by X. Then, the pixel values of cover image are denoted by $(p_1, p_2, p_3, \dots\dots\dots, p_M)$ and $j-$ th pixel value of the cover image is denoted as p_j. Total number of pixels present in the cover image are denoted by M which implies $|X| \to M$. Consider that the respective estimated pixel values are denoted as $\hat{p}_j$ which is determined using image pixel estimation function$(\cdot)$ where $j = 1,2,3, \dots\dots\dots, M$. Then,

$\hat{p}_j = \text{Estimated}\left(X_j\right)$	(1)

Where, X_j is determined as the subset of pixels utilized to estimate $j-$ th pixel value i.e.$X_j \subseteq X$. Generally, X_j contains pixels adjacent to the $j-$ th pixel and precise location of associate pixels

depends upon the image pixel estimation function. Further, determined the estimation error g_j with respect to p_j as follows,

$$g_j = p_j - \hat{p}_j$$	(2)

Then, determine the histogram of estimated errors g_j. Here, the histogram of estimated errors are evaluated by dividing group of estimated errors where every group precisely belongs to value of one pixel estimated error respectively. Every estimated error value $R(i)$ of the partition is the cardinality of group of pixel estimated error values i for histogram evaluation, where $R(i)$ lies in the range $0 \leq R(i) \leq M$. Then,

$$R(i) = \left\lvert \{ g_j : g_j = i, j = 1,2,3 \dots \dots \dots, M \} \right\rvert$$	(3)

Where, cardinality of group H is expressed by $|H|$. For an instance, an 8 bit gray scale image with a resolution of 512×512, cardinality lies in a range of $0 \leq R(i) \leq 262144$. Then, apply embedded method by shifting of estimated errors g_j,

$$g_j' = 2g_j + c \text{ if } g_j \in [-L, L]$$	(4)

Then, by simplifying equation (4), we get,

$$g_j' = g_j + c \text{ if } g_j \in [L, +\infty]$$ $$g_j' = g_j - L \text{ if } g_j \in [-\infty, -L]$$	(5)

Where, c is watermark bit which need to be embedded for $j = 1,2,3, \dots \dots \dots, M$ and lies in the range $c \in \{0,1\}$. Here, L is expressed as the threshold embedded coefficient to handle the embedded capacity. Then, the estimated errors which lies in the range $[-L, L)$ are extended for embedding of estimated errors to obtain histogram of estimated errors. Moreover, the estimated errors outside the mentioned range are discarded and shifted outside of their neighborhood. Lastly, the improvised error g_j' is summed with estimated pixel value $\hat{p}_j$ to obtain watermarked pixel series p_j',

$$p_j' = \hat{p}_j + g_j'$$	(6)

3.2 Retrieval Method of Reduction of Error Estimation (REE):

By using similar estimation method, the estimated value $\widehat{p_j'}$ to every watermarked pixel p_j' respectively for $j = 1,2,3, \ldots \ldots \ldots, M$ is determined by,

$\widehat{p_j'} = \text{Estimated}\left(X_j'\right)$	(7)

Where, X_j' contains pixels adjacent to the $j-\text{th}$ watermarked pixel i.e. p_j'. Then, the estimated error g_j' for $j = 1,2,3, \ldots \ldots \ldots, M$ determined by following equation,

$g_j' = p_j' - \widehat{p_j'}$	(8)

Then, the original estimated error recovered from watermarked estimated error for $j = 1,2,3, \ldots \ldots \ldots, M$ is given by following equation,

$g_j = \lfloor g_j'/2 \rfloor \quad \text{if } g_j' \in [-2L, 2L]$ $g_j = g_j' - c \text{ if } g_j' \in [2L, +\infty]$ $g_j = g_j' + L \text{ if } g_j' \in [-\infty, -2L]$	(9)

Then, retrieved pixels of cover image for $j = 1,2,3, \ldots \ldots \ldots, M$ isgiven by following equation,

$p_j = \widehat{p_j'} - g_j$	(10)

Lastly, the watermark bits retrieved as,

$c = g_j' - 2\left\lfloor \frac{g_j'}{2} \right\rfloor \quad \text{if } g_j' \in [-2L, 2L)$	(11)

3.3 Mean Bias for Reduction of Error Estimation (REE):

In above section it discussed that estimated errors lies in the range $[-L, L)$ for Reduction of Error Estimation (REE) mechanism obtained with the help of proposed reversible watermarking technique are extended and then permitted to embed watermark bits. Then, embedding capacity is expressed as,

$$D = \sum_{i=-L}^{L-1} R(i) \quad (12)$$

Where, R is expressed as histogram of estimated error and R(i) is represented as the total number of incidence of estimated error i. Then, after embedding, estimated errors g_j which lies in the range $[-L, L)$ may have Bias to a minor extent. The Bias presence rely upon the type of watermarked used. However, due to continuous shifting, estimated errors g_j which are placed outside the range of $[-L, L)$ i.e. $g_j \in (-\infty, -L) \cup [L, \infty)$ have a fixed Bias. The magnitude of fixed Bias of estimated errors g_j in the range $g_j \in (-\infty, -L) \cup [L, \infty)$ is denoted as L. Then, after square of Bias in estimated error is given by,

$$N(p_j, p_j') = \left\| p_j - p_j' \right\|^2 \quad (13)$$

Then, mean Bias of estimated error for $j-$ th pixel is represented by following equation,

$$N(p_j, p_j') = \left\| p_j - p_j' \right\|^2 = \left\| e_j - e_j' \right\|^2 = \begin{cases} \frac{1}{2} \sum_{c \in \{0,1\}} (g_j + c)^2 = g_j^2 + g_j + \frac{1}{2} & \text{if} g_j \in [-L, L) \\ L^2 & \text{otherwise} \end{cases} \quad (14)$$

Therefore, the mean Bias is given by,

$$N_{mean} = \sum_{i=-L}^{L-1} \left(i^2 + i + \frac{1}{2} \right) R(i) + \left(\sum_{i=-\infty}^{-L-1} R(i) + \sum_{i=L}^{+\infty} R(i) \right) L^2 \quad (15)$$

Here, it is evident that in embedding considering case of watermarking or reversible watermarking, the Bias and capacity remain similar for the histogram values of estimated errors. However, their respective weights can be changed.

3.4 Optimization of Information Loss Minimization (ILM) Problem:

Here, optimum linear filtering methods are adopted to optimize Information Loss Minimization (ILM) Problem. Then, ILM problem is formulated in following way,

$$\min(c_1 p_1 + c_2 p_2 + \ldots\ldots\ldots + c_M p_M) \quad (16)$$

Such that : $h_{11}p_1 + h_{12}p_2 + \ldots\ldots + h_{1M}p_M \geq I_1$ $h_{21}p_1 + h_{22}p_2 + \ldots\ldots + h_{2M}p_M \geq I_2$ $\vdots$ $h_{M1}p_1 + h_{M2}p_2 + \ldots\ldots + h_{MM}p_M \geq I_M$	

Where, the coefficients c_j, h_{je}, p_j need to be evaluated and here, $I_j \in Y$ for $j = 1,2,3, \ldots\ldots\ldots, M$. Then, the Information Loss Minimization (ILM) problem for Reduction of Error Estimation (REE) using reversible watermarking and optimum linear filtering method is given by,

$\min\ N_{mean}, \quad \text{subject to: } D - d \geq 0$	(17)

Where, d represents a positive constant coefficient which demonstrates size of payload and embedding capability of cover image is given by D. Then, after multiplying the average function by 2 gives,

$\min\ 2N_{mean}, \quad \text{subject to: } D - d \geq 0$	(18)

Then, assume a specific range as $[-L_\infty, L_\infty]$for histogram of estimated errors where $-L_\infty$ and L_∞ are threshold limits of embedding operation. Consider that the real threshold limits for embedding operation is $[-L, L)$. Then, embedding capability D of estimated error values is represented as the linear arrangement for histogram values of estimated errors. Then, mean Bias is represented as the shifted histogram values of estimated errors with fixed Bias. Thus,

$D = \sum_{j=-L_\infty}^{L_\infty} d_j R(j) \text{ and } 2N_{mean} = \sum_{j=-L_\infty}^{L_\infty} n_j R(j)$	(19)

Further, compare above expressions in equation (19) with equation (12) and equation (14),

$d_j = \begin{cases} 1 & \text{if } j \in [-L, L) \\ 0 & \text{otherwise} \end{cases}$	(20)

And,

$$n_j = \begin{cases} 2j^2 + 2j + 1 \\ 2L^2 \quad \text{otherwise} \end{cases} \tag{21}$$

Where, the coefficients d_j and n_j lies in a range $d_j, n_j \in [0, \infty]$. Then, these coefficients are evaluated for a threshold embedding coefficient L in polynomial time. Therefore, ILM problem is minimized by placing values of equation (22) in equation (16),

$$c_j = n_j \tag{22}$$

$$h_{1j} = d_j$$

$$h_{jj} = 1 \quad 2 \le j \le M$$

$$h_{je} = 0 \quad 2 \le j \le M, j \ne e$$

$$p_j = R(j)$$

$$I_1 = d$$

$$I_j = 0 \quad 2 \le j \le M$$

As the substitution of values in equation (16) take place in polynomial time. Therefore, Information Loss Minimization (ILM) Problem is NP-hard problem as well as their decision model also contain NP-hard problem.

3.5 Optimization of Reversible Watermarking Capacity Enhancement (RWCE) Problem:

Here, optimum linear filtering method is analysed as well as their complexity. Assume that there are m items, the filtering capacity is denoted by F, and then the value of $j-th$ item is w_j and their respective weight is v_j. Here, all the coefficients w_j, v_j and F are integers. Then, Reversible Watermarking Capacity Enhancement (RWCE) Problem can be formulated by following equation,

$$\max \sum_{j=1}^{m} w_j p_j \tag{23}$$

Such that: $\sum_{j=1}^{m} v_j p_j \le F, \quad p_j \in \{0\} \cup \mathbb{Q}^+$

Where, the coefficient p_j lies in a range $p_j \in [0, \infty]$ and utilized to magnify the value of objective function for $j-th$ item. Then, the Reversible Watermarking Capacity Enhancement (RWCE) problem for Reduction of Error Estimation (REE) using reversible watermarking and optimum linear filtering method is given by,

$$\max D, \quad \text{subject to: } N_{mean} - n \leq 0 \tag{24}$$

Where, d represents a positive constant coefficient which demonstrates Bias limit. Then, after multiplying the Bias limit function by 2 gives,

$$\max D, \quad \text{subject to: } 2N_{mean} - 2n \leq 0 \tag{25}$$

Then, embedding capability D and mean Bias N_{mean} of estimated error values is represented as the linear arrangement for histogram values of estimated errors. Here, the coefficients d_j and n_j are evaluated from equation (20) and (21). Moreover, it is evident that the histogram values of estimated errors R(j) which lies in the range $j \in (-L_{\infty}, -L) \cup [L, L_{+\infty})$ are not able to contribute to the embedding capability D. However, they produces a fixed Bias of $2L^2$ to the mean Bias N_{mean}. Then, maximization of embedding capability D for a fixed Bias of $2L^2$ is given by,

$$R(j) = 0 \quad \ncong \forall_j \in (-L_{\infty}, -L) \cup [L, L_{+\infty}) \tag{26}$$

Therefore, the embedding capability D and mean Bias N_{mean} is simplified by following equation,

$$D = \sum_{j=-L}^{L-1} d_j R(j) \text{ and } 2N_{mean} = \sum_{j=-L}^{L-1} n_j R(j) \tag{27}$$

Thus, Optimization of Reversible Watermarking Capacity Enhancement (RWCE) Problem is achieved as,

$$\max \sum_{j=-L}^{L-1} d_j R(j) \tag{28}$$

Such that: $\sum_{j=-L}^{L-1} n_j R(j) \leq 2n$

Then, then the RWCE Problem is minimized as,

$p_j = R(j), \quad w_j = d_j, \quad v_j = n_j, \quad F = 2n$	(29)

The change take place in polynomial time. Therefore, Reversible Watermarking Capacity Enhancement (RWCE) Problem is NP-hard problem as well as their decision model also contain a NP-hard problem.

4 Result and Discussion:

This section discusses about the performance results of the proposed reversible watermarking technique based on Optimum linear filtering algorithms and compared with several state-of-art-watermarking techniques. Here, proposed reversible watermarking technique minimizes Information Loss Minimization (ILM) Problem for Reduction of Error Estimation (REE) as well as determines nature of problem as NP-hard problem to improve the efficiency of the model. Similarly, the proposed model also minimizes Reversible Watermarking Capacity Enhancement (RWCE) Problem for REE to enhance performance efficiency and nature of the problem is determined as NP-hard problem. Here, modelling for embedding and retrieval of REE as well as amount of Bias occur between both the processes are determined. Along with that optimization of the ILM and RWCE problem is achieved based on Optimum linear filtering algorithm which improves performance efficiency of proposed reversible watermarking technique.

The performance of proposed reversible watermarking is tested on several medical images like MRI images, Fundus images and CT scan image which are utilized as cover images in watermarking process. Here, proposed reversible watermarking technique efficiently authenticate medical image by fusing cover image with watermarked image. Along with that, proposed model precisely identify localization of tempered region in case of various attacks as well as recover tempered information as original image after attacks. Therefore, proposed reversible watermarking technique is capable of handling different functionalities with improved efficiency results compare to various state-of-art-watermarking technique. Performance efficiency of the proposed model is evaluated based on the performance metrics like Peak Signal to Noise Ratio (PSNR), Structure Similarity Measure Index (SSIM), Bit Error Rate (BER) and Normalized Cross Correlation (NCC). Furthermore, mean of these performance metrics for varied medical images are evaluated to compare with several traditional watermarking techniques under various attacks. These attacks are Average Filtering (AF), Gaussian Blurring (GB), Gaussian Noise (GN), JPEG compression (JC), JPEG2000 compression, Median Filtering (MF), Cropping from image edges (CR), Salt and Pepper Noise (SN), Resizing (RS) and Weiner Filtering (WF). All these attacks have their own different evaluation parameters to determined performance metric results under their respective attack and then, compared with traditional watermarking algorithms.

Here, Table 1 demonstrates mean results considering PSNR and SSIM using proposed reversible watermarking algorithms and compared against several traditional watermarking methods like Maheshakar et. al [24], Thabit et. al [25], Lei.et.al [26], Thabit et. al. [27], Xiyao et.

al. [13]. The mean PSNR evaluated using proposed reversible watermarking technique is 56.5604. Here, PSNR results obtained from proposed model is slightly higher than Maheshakar et. al [24] and Thabit et. al [25] whereas proposed model is comparatively better than Lei.et.al [26], Thabit et. al. [27] and Xiyao et. al. [13] in terms of PSNR. Similarly, mean SSIM result using proposed reversible watermarking technique under various attacks is 0.9991. Mean SSIM obtained using proposed model outperforms all the traditional techniques such as Maheshakar et. al [24], Thabit et. al [25], Lei.et.al [26], Thabit et. al. [27], Xiyao et. al. [13]. The reason behind high performance is the utilization of Optimum linear filtering algorithm to minimize ILM and RWCE problem. Results demonstrated considering mentioned performance metrics for authenticity measure, temper localization measure and temper retrieval under various attacks concludes the superiority of proposed reversible watermarking technique and proposed model outperforms all the traditional watermarking methods in terms of PSNR, SSIM, BER and NCC.

Table 1 mean PSNR and mean SSIM Results comparison with various state-of-art-watermarking techniques

Algorithms	**PSNR**	**SSIM**
Maheshakar et. al [24]	39.7522	0.9669
Thabit et. al [25]	40.1841	0.9607
Lei.et.al [26]	41.5525	0.9660
Thabit et. al. [27]	42.8972	0.9670
Xiyao et. al. [13]	41.2995	0.9607
Proposed Reversible Watermarking	**51.1604**	**0.9991**

Furthermore, 10 types of common different attacks are demonstrated in Table 2 to test the efficiency and robustness of proposed reversible watermarking technique. Furthermore, proposed reversible watermarking technique is compared against five traditional watermarking algorithms [24], [25], [26], [27] and [13] to conclude imperceptibility and robustness of proposed model. Performance metrics like mean NCC and mean BER are evaluated under various conditions like in case of data authenticity, temper localization and temper recovery which is demonstrated in Table 3, Table 4 and Table 5. Here, Table 3 shows all the mean NCC results are nearly 1 and all the mean BER results are nearly 0 under the condition of data authenticity considering various attacks. Table 3 demonstrates reliable authenticity results compare to several traditional watermarking methods. Furthermore, the average of mean NCC value obtained under all attacks using proposed model is **0.9787** is higher compare to traditional watermarking methods like Maheshakar et. al [24], Thabit et. al [25], Lei.et.al [26], Xiyao et. al. [13] which obtain NCC results as 0.9322, 0.9362, 0.8702 and 0.9562. Similarly, the average of mean BER value obtained under all attacks using proposed model is **0.0114** is lower compare to traditional watermarking methods

like Maheshakar et. al [24], Thabit et. al [25], Lei.et.al [26], Xiyao et. al. [13] which obtain BER results as 0.0927, 0.0711, 0.1003 and 0.0462.

Here, Table 4 shows all the mean NCC results are nearly 1 and all the mean BER results are nearly 0 under the condition of temper localization considering various attacks. Table 4 demonstrates reliable temper localization results compare to several traditional watermarking methods. Furthermore, the average of mean NCC value obtained under all attacks using proposed model is **0.9967** is higher compare to traditional watermarking methods like Maheshakar et. al [24], Thabit et. al [25], Lei.et.al [26], Xiyao et. al. [13] which obtain NCC results as 0.9322, 0.9362, 0.8702 and 0.9562. Similarly, the average of mean BER value obtained under all attacks using proposed model is **0.0148** is lower compare to traditional watermarking methods like Maheshakar et. al [24], Thabit et. al [25], Lei.et.al [26], Xiyao et. al. [13] which obtain BER results as 0.0927, 0.0711, 0.1003 and 0.0462.

Table 2 Attacks with Parameters

Attack Type	**Parameters**	**Attack Type**	**Parameters**
Average Filtering (AF)	Window= 3x3,5x5	Median Filtering (MF)	Window= 3x3,5x5
Gaussian Blurring (GB)	Window=3x3, variance=0.5,1	Cropping from image edges (CR)	5%, 10% and 20%
Gaussian Noise (GN)	Variance= 0.0001, Mean= 0.001,0.003,0.0005	Salt and Pepper Noise (SN)	Density = 0.001,0.003, 0.0005
JPEG compression (JC)	Quality = 70,80	Resizing (RS)	0.8,1.2
JPEG2000 compression	Compression Ratio= 4,8	Weiner Filtering (WF)	Window= 3x3,5x5

Here, Table 5 shows all the mean NCC results are nearly 1 and all the mean BER results are nearly 0 under the condition of temper information retrieval considering various attacks. Table 5 demonstrates reliable temper information retrieval results compare to several traditional watermarking methods. Furthermore, the average of mean NCC value obtained under all attacks using proposed model is **0.9967** is higher compare to traditional watermarking methods like Maheshakar et. al [24], Thabit et. al [25], Lei.et.al [26], Xiyao et. al. [13] which obtain NCC results as 0.9322, 0.9362, 0.8702 and 0.9562. Similarly, the average of mean BER value obtained under all attacks using proposed model is **0.0144** is lower compare to traditional watermarking methods like Maheshakar et. al [24], Thabit et. al [25], Lei.et.al [26], Xiyao et. al. [13] which obtain BER results as 0.0927, 0.0711, 0.1003 and 0.0462.

The reason behind high performance efficiency under all three scenarios is efficient embedding and retrieval process of REE and optimization of the ILM and RWCE problem using Optimum linear filtering algorithm. However, mean NCC and mean BER under data authenticity are slightly higher which are demonstrated in Table 3 than the mean NCC and mean BER under temper localization and temper information retrieval which are demonstrated in Table 4 and Table 5 respectively. It is evident from the performance metric result of Table 1, Table 3, Table 4 and Table 5 that all the result of performance metrics outperforms above mentioned state-of-art-watermarking techniques in terms of PSNR, SSIM, BER and NCC under all three scenarios as for data authenticity, temper localization and temper information retrieval. Along with that, Figure 1 demonstrates the visual representation of original medical images and watermarked medical images. Here, total five types of medical images are taken to evaluate performance results of proposed reversible watermarking technique. There are total number of 200 images are present in the dataset in which the number of CT scan images are 40, MRI images are 40, X-ray images are 40, fundus image are 40 and remaining 40 images are Ultrasound images. Here, five type of varied medical images are watermarked using a hospital logo with a pixel resolution of 256×256. This hospital logo image is utilized as authenticity data as demonstrated in Figure 1. Furthermore, the superiority of proposed reversible watermarking technique is evident from visual representation results of Figure 1.

Table 3 the mean BERs and NCCs of authenticity data under various attacks

Attacks	**Maheshakar et. al [24]**		**Thabit et. al [25]**		**Lei.et.al [26]**		**Thabit et. al. [27]**		**Xiyao et. al. [13]**		**Proposed Model**	
	BER	**NCC**	**BER**	**NCC**	**BER**	**NCC**	**BER**	**NCC**	**BER**	**NCC**	**BER**	**NCC**
AF (3x3)	0.1071	0.8868	0.0622	0.9463	0.1485	0.8132	0.0146	0.9844	0.0705	0.9604	0.0083	0.9841
AF(5x5)	0.2425	0.7831	0.3353	0.6953	0.2659	0.6955	0.1424	0.8543	0.1371	0.8978	0.0060	0.9883
MF(3x3)	0.0866	0.9915	0.0539	0.9549	0.1039	0.8557	0.0162	0.9823	0.0457	0.9759	0.0133	0.9749
MF(5x5)	0.2353	0.7934	0.3807	0.6538	0.2170	0.7369	0.2138	0.7793	0.1098	0.9215	0.0103	0.9803
GB (0.5)	0.0162	0.9797	0.0000	1.0000	0.0217	0.9780	0.0000	1.0000	0.0094	0.9937	0.0311	0.9442
GB (1)	0.1064	0.8733	0.0491	0.9585	0.1671	0.7963	0.0031	0.9965	0.0914	0.9422	0.0311	0.9441
CR (5%)	0.0361	0.9879	0.0058	0.9956	0.0526	0.9081	0.0138	0.9816	0.0000	1.0000	0.0310	0.9443
CR (10%)	0.0793	0.9844	0.0130	0.9836	0.1051	0.8061	0.0610	0.8980	0.0000	1.0000	0.0120	0.9773

CR (20%)	0.1538	0.9842	0.0424	0.9455	0.1907	0.6402	0.1558	0.7643	0.0644	0.9803	0.0141	0.9736
GN (0.001)	0.0722	0.9273	0.0001	0.9993	0.0578	0.9357	0.0011	0.9990	0.0117	0.9885	0.0116	0.9781
GN(0.003)	0.0730	0.9268	0.0009	0.9993	0.1779	0.8116	0.0012	0.9989	0.0721	0.9016	0.0070	0.9864
GN(0.005)	0.0733	0.9260	0.0011	0.9991	0.2072	0.7818	0.0013	0.9987	0.1349	0.8723	0.0092	0.9824
SN(0.001)	0.0565	0.9791	0.0242	0.9786	0.0220	0.9386	0.0051	0.9950	0.0282	0.9744	0.0067	0.9870
SN(0.003)	0.0691	0.9642	0.0684	0.9399	0.0611	0.9386	0.0142	0.9855	0.0758	0.9306	0.0160	0.9703
SN(0.005)	0.0808	0.9493	0.1013	0.9100	0.0971	0.9023	0.0240	0.9758	0.1246	0.8866	0.0044	0.9913
JC (Q=70)	0.1062	0.9700	0.1294	0.8806	0.0155	0.9842	0.0422	0.9851	0.0061	0.9939	0.0018	0.9965
JC(Q=80)	0.0940	0.9721	0.0470	0.9577	0.0048	0.9955	0.0025	0.9970	0.0032	0.9982	0.0009	0.9981
JPEG2000 (4)	0.0475	0.9755	0.0012	0.9988	0.0021	0.9979	0.0044	0.9961	0.0023	0.9993	0.0016	0.9967
JPEG2000 (8)	0.0851	0.9539	0.0227	0.9819	0.0239	0.9616	0.0401	0.9638	0.0133	0.9874	0.0007	0.9986
RS (0.8)	0.0265	0.9683	0.0035	0.9975	0.0255	0.9654	0.0001	0.9999	0.0057	0.9972	0.0164	0.9696
RS (1.2)	0.0080	0.9906	0.0001	1.0000	0.0069	0.9934	0.0000	1.0000	0.0010	0.9988	0.0137	0.9743
WF (3x3)	0.0787	0.9203	0.0539	0.9662	0.1000	0.8629	0.0130	0.9871	0.0122	0.9935	0.0096	0.9815
WF (5x5)	0.1977	0.8320	0.2347	0.7911	0.2333	0.7280	0.0704	0.9250	0.0757	0.9412	0.0056	0.9891
Average	**0.0927**	**0.9322**	**0.0711**	**0.9362**	**0.1003**	**0.8702**	**0.0365**	**0.9586**	**0.0476**	**0.9624**	**0.0114**	**0.9787**

Table 4 the mean BERs and NCCs of tamper localization information under various attacks.

Attacks	**Maheshakar et. al [24]**		**Thabit et. al [25]**		**Lei.et.al [26]**		**Thabit et. al. [27]**		**Xiyao et. al. [13]**		**Proposed Model**	
	BER	**NCC**	**BER**	**NCC**	**BER**	**NCC**	**BER**	**NCC**	**BER**	**NCC**	**BER**	**NCC**

AF (3x3)	0.4957	0.5041	0.4707	0.5134	N/A	N/A	N/A	N/A	0.0478	0.9541	0.0116	0.9918
AF(5x5)	0.5018	0.5006	0.4852	0.5001	N/A	N/A	N/A	N/A	0.1422	0.8525	0.0139	0.9846
MF(3x3)	0.3259	0.6695	0.4220	0.5641	N/A	N/A	N/A	N/A	0.0250	0.9687	0.0055	0.9990
MF(5x5)	0.5666	0.5632	0.5349	0.5007	N/A	N/A	N/A	N/A	0.1038	0.8900	0.0108	0.9941
GB (0.5)	0.4413	0.5581	0.0132	0.9862	N/A	N/A	N/A	N/A	0.0041	0.9944	0.0519	0.9993
GB (1)	0.4969	0.5028	0.2030	0.7907	N/A	N/A	N/A	N/A	0.0681	0.9322	0.0432	0.9993
CR (5%)	0.0124	0.9739	0.0223	0.9661	N/A	N/A	N/A	N/A	0.0000	1.0000	0.0545	0.9993
CR (10%)	0.0347	0.9273	0.0549	0.9097	N/A	N/A	N/A	N/A	0.0000	1.0000	0.0209	0.9990
CR (20%)	0.0812	0.8320	0.1668	0.7827	N/A	N/A	N/A	N/A	0.0627	0.8901	0.0199	0.9993
GN (0.001)	0.4977	0.5018	0.1101	0.8843	N/A	N/A	N/A	N/A	0.0103	0.9948	0.0124	0.9998
GN(0.003)	0.4979	0.5017	0.1102	0.8839	N/A	N/A	N/A	N/A	0.0587	0.9868	0.0163	0.9995
GN(0.005)	0.4999	0.5013	0.1112	0.8830	N/A	N/A	N/A	N/A	0.1395	0.9329	0.0099	0.9917
SN(0.001)	0.0006	0.9994	0.0261	0.9710	N/A	N/A	N/A	N/A	0.0358	0.9651	0.0133	0.9831
SN(0.003)	0.0015	0.9986	0.0649	0.9303	N/A	N/A	N/A	N/A	0.0970	0.9031	0.0035	1.0000
SN(0.005)	0.0026	0.9973	0.0959	0.8976	N/A	N/A	N/A	N/A	0.1397	0.8521	0.0032	1.0000
JC (Q=70)	0.4960	0.5036	0.4130	0.5706	N/A	N/A	N/A	N/A	0.0057	0.9965	0.0029	1.0000
JC(Q=80)	0.4931	0.5066	0.3564	0.6293	N/A	N/A	N/A	N/A	0.0041	0.9975	0.0041	0.9970
JPEG2000 (4)	0.2886	0.7107	0.0682	0.9296	N/A	N/A	N/A	N/A	0.0015	0.9985	0.0051	0.9919
JPEG2000 (8)	0.4565	0.5433	0.2527	0.7359	N/A	N/A	N/A	N/A	0.0088	0.9956	0.0039	0.9985

RS (0.8)	0.4709	0.5288	0.0980	0.8994	N/A	N/A	N/A	N/A	0.0026	0.9973	0.0034	1.0000
RS (1.2)	0.4009	0.5988	0.0175	0.9819	N/A	N/A	N/A	N/A	0.0008	0.9992	0.0039	0.9999
WF (3x3)	0.4908	0.6695	0.4220	0.5697	N/A	N/A	N/A	N/A	0.0113	0.9868	0.0116	0.9991
WF (5x5)	0.5007	0.5632	0.4345	0.5505	N/A	N/A	N/A	N/A	0.0929	0.9043	0.0140	0.9983
Average	**0.3502**	**0.6590**	**0.2154**	**0.7752**	**N/A**	**N/A**	**N/A**	**N/A**	**0.0462**	**0.9562**	**0.0148**	**0.9967**

Table 5 the mean BERs and NCs of tamper recovery information under various attacks.

Attacks	**Maheshakar et. al [24]**		**Thabit et. al [25]**		**Lei.et.al [26]**		**Thabit et. al. [27]**		**Xiyao et. al. [13]**		**Proposed Model**	
	BER	**NCC**	**BER**	**NCC**	**BER**	**NCC**	**BER**	**NCC**	**BER**	**NCC**	**BER**	**NCC**
AF (3x3)	0.1043	0.8909	0.4240	0.4813	0.14	0.81	0.01	0.98	0.0397	0.9592	0.0116	0.9925
AF(5x5)	0.2377	0.7864	0.4740	0.4337	N/A	N/A	N/A	N/A	0.1508	0.8490	0.0139	0.9846
MF(3x3)	0.0838	0.9162	0.3724	0.5390	N/A	N/A	N/A	N/A	0.0254	0.9726	0.0057	0.9989
MF(5x5)	0.2300	0.7974	0.4785	0.4332	N/A	N/A	N/A	N/A	0.1114	0.8836	0.0108	0.9939
GB (0.5)	0.0154	0.9815	0.0163	0.9759	N/A	N/A	N/A	N/A	0.0044	0.9963	0.0506	0.9995
GB (1)	0.1046	0.8781	0.2202	0.7200	N/A	N/A	N/A	N/A	0.0607	0.9402	0.0417	0.9994
CR (5%)	0.0348	0.9874	0.0329	0.9357	N/A	N/A	N/A	N/A	0.0000	1.0000	0.0533	0.9995
CR (10%)	0.0759	0.9852	0.0849	0.8320	N/A	N/A	N/A	N/A	0.0000	1.0000	0.0196	0.9990
CR (20%)	0.1490	0.9845	0.2100	0.6919	N/A	N/A	N/A	N/A	0.0498	0.9183	0.0186	0.9994
GN (0.001)	0.0666	0.9327	0.1043	0.8540	N/A	N/A	N/A	N/A	0.0059	0.9950	0.0120	0.9999
GN(0.003)	0.0670	0.9323	0.1200	0.8538	N/A	N/A	N/A	N/A	0.0598	0.9860	0.0159	0.9996

GN(0.005)	0.0677	0.9315	0.1250	0.8531	N/A	N/A	N/A	N/A	0.1010	0.9486	0.0099	0.9916
SN(0.001)	0.0535	0.9802	0.0279	0.9584	N/A	N/A	N/A	N/A	0.0390	0.9599	0.0132	0.9831
SN(0.003)	0.0662	0.9651	0.0692	0.8999	N/A	N/A	N/A	N/A	0.1056	0.8935	0.0039	1.0000
SN(0.005)	0.0782	0.9508	0.0750	0.8498	N/A	N/A	N/A	N/A	0.1552	0.8373	0.0031	1.0000
JC (Q=70)	0.0974	0.9716	0.3785	0.5337	N/A	N/A	N/A	N/A	0.0043	0.9946	0.0028	1.0000
JC(Q=80)	0.0865	0.9732	0.3087	0.6147	N/A	N/A	N/A	N/A	0.0031	0.9957	0.0035	0.9970
JPEG2000 (4)	0.0452	0.9774	0.0750	0.9351	N/A	N/A	N/A	N/A	0.0020	0.9969	0.0046	0.9920
JPEG2000 (8)	0.0789	0.9564	0.2650	0.7258	N/A	N/A	N/A	N/A	0.0058	0.9941	0.0033	0.9985
RS (0.8)	0.0249	0.9705	0.1071	0.8645	N/A	N/A	N/A	N/A	0.0029	0.9975	0.0039	1.0000
RS (1.2)	0.0075	0.9915	0.0213	0.9704	N/A	N/A	N/A	N/A	0.0007	0.9992	0.0042	1.0000
WF (3x3)	0.0761	0.9233	0.4100	0.5187	N/A	N/A	N/A	N/A	0.0112	0.9867	0.0117	0.9990
WF (5x5)	0.1932	0.8336	0.4161	0.4927	N/A	N/A	N/A	N/A	0.1099	0.8873	0.0140	0.9982
Average	**0.0889**	**0.9346**	**0.2049**	**0.7377**	**N/A**	**N/A**	**N/A**	**N/A**	**0.0456**	**0.9562**	**0.0144**	**0.9967**

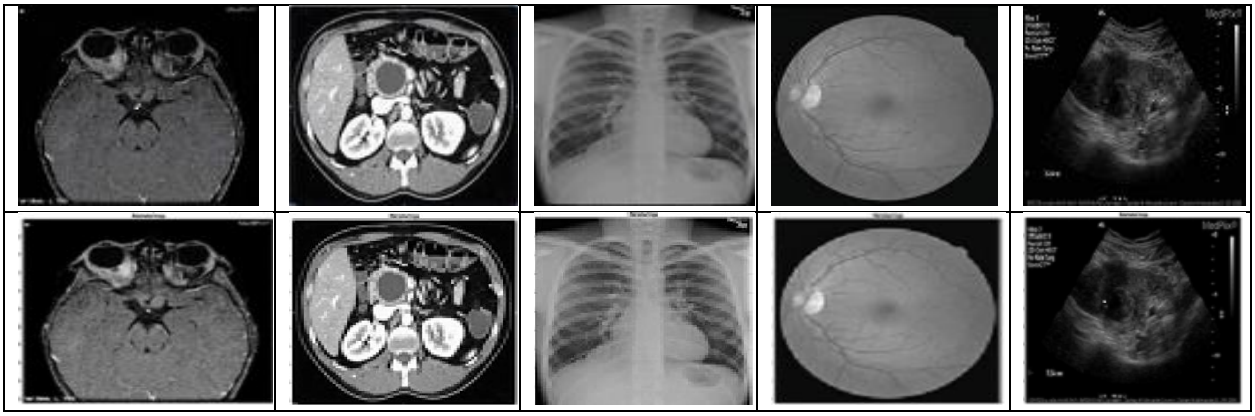

Figure 1 Examples of evaluating the watermarking imperceptibility. First row shows original medical images, second rows shows watermarked medical images.

5 Conclusion:

The importance of watermarking schemes while diagnosis and sharing with other radiologists or experts is extremely high due to possibility of patient's data tempering. Therefore, a Reversible Watermarking Technique is employed to authenticate medical images like CT scan images, X-rays, fundus images, MRI in this article. Highly efficient watermarking is achieved with the help of Optimum linear filtering algorithms. First of all, embedding for Reduction of Error Estimation (REE) is achieved and then pixels of cover images are retrieved as original for Reduction of Error Estimation (REE) and then Bias occur between both the processes are evaluated using Optimum linear filtering methods. Along with that, the proposed reversible watermarking scheme optimizes Information Loss Minimization (ILM) Problem and Reversible Watermarking Capacity Enhancement (RWCE) Problem and also determines nature of the problem as NP-hard. Thus, performance efficiency of proposed watermarking model is improved due to reduction of complexity and NP-hard problem. A detailed mathematical modelling to achieve highly efficient reversible watermarking is presented. Furthermore, Average of mean SSIM value obtained under all attacks using proposed model is **0.9991** and mean PSNR is **51.1604** which is higher than several state-of-art-watermarking techniques. All the result of performance metrics outperforms above mentioned state-of-art-watermarking techniques in terms of PSNR, SSIM, BER and NCC under all three scenarios as for data authenticity, temper localization and temper information retrieval.

References:

[1]	Q. Yao, Y. Tian, P.-F. Li, L.-L. Tian, Y.-M. Qian, and J.-S. Li, ``Design and development of a medical big data processing system based on Hadoop," J. Med. Syst., vol. 39, no. 3, pp. 1_11, Feb. 2015.
[2]	J. C. Dagadu and J. Li, ``Context-based watermarking cum chaotic encryption for medical images in telemedicine applications," Multimedia Tools Appl., vol. 77, no. 18, pp. 24289_24312, 2018.
[3]	A. Bakshi and A. K. Patel, ``Secure telemedicine using RONI halftoned visual cryptography without pixel expansion," J. Inf. Secur. Appl., vol. 46, pp. 281_295, Jun. 2019, doi: 10.1016/j.jisa.2019.03.004.
[4]	A. Ustubioglu and G. Ulutas, ``A new medical image watermarking tech- nique with _ner tamper localization," J. Digit. Imag., vol. 30, no. 6, pp. 665_680, Dec. 2017.
[5]	H. Nyeem, W. Botes, and C. Boyd, ``A review of medical image water- marking requirements for technology," J. Digit. Imag., vol. 26, no. 2, pp. 326_343, 2013.
[6]	S. Alam, A. Jamil, A. Saldhi, and M. Ahmad, ``Digital image authentication and encryption using digital signature," in Proc. Int. Conf. Adv. Comput. Eng. Appl. (ICACEA), Ghaziabad, India, Mar. 2015, pp. 332_336.
[7]	O. Hemida and H. He, ``A self-recovery watermarking scheme based on block truncation coding and quantum chaos map," Multimedia Tools Appl., vol. 79, pp. 18695_18725, Jan. 2020, doi: 10.1007/s11042-020-08727-7.

[8]	J. Molina-Garcia, B. P. Garcia-Salgado, V. Ponomaryov, R. Reyes-Reyes, S. Sadovnychiy, and C. Cruz-Ramos, ``An effective fragile watermarking scheme for color image tampering detection and self-recovery," Signal Process., Image Commun., vol. 81, Feb. 2020, Art. no. 115725.
[9]	O. M. Al-Qershi and B. E. Khoo, ``Authentication and data hiding using a reversible ROI-based watermarking scheme for DICOM images," in Proc. Int. Conf. Med. Syst. Eng. (ICMSE), 2009, pp. 829_834.
[10]	X. Deng, Z. Chen, F. Zeng, Y. Zhang, and Y. Mao, ``Authentication and recovery of medical diagnostic image using dual reversible digital watermarking," J. Nanosci. Nanotechnol., vol. 13, no. 3, pp. 2099_2107, Mar. 2013.
[11]	X. Luo, Q. Cheng, and J. Tan, ``A lossless data embedding scheme for medical images in application of e-diagnosis," in Proc. 25th Annu. Int. Conf. IEEE Eng. Med. Biol. Soc., Sep. 2003, pp. 852_855.
[12]	N. A. Memon and A. Alzahrani, "Prediction-Based Reversible Watermarking of CT Scan Images for Content Authentication and Copyright Protection," in IEEE Access, vol. 8, pp. 75448-75462, 2020, doi: 10.1109/ACCESS.2020.2989175.
[13]	X. Liu et al., "A Novel Robust Reversible Watermarking Scheme for Protecting Authenticity and Integrity of Medical Images," in IEEE Access, vol. 7, pp. 76580-76598, 2019, doi: 10.1109/ACCESS.2019.2921894.
[14]	G. -D. Su, C. -C. Chang and C. -C. Lin, "Effective Self-Recovery and Tampering Localization Fragile Watermarking for Medical Images," in IEEE Access, vol. 8, pp. 160840-160857, 2020, doi: 10.1109/ACCESS.2020.3019832.
[15]	J. Liu, J. Ma, J. Li, M. Huang, N. Sadiq and Y. Ai, "Robust Watermarking Algorithm for Medical Volume Data in Internet of Medical Things," in IEEE Access, vol. 8, pp. 93939-93961, 2020, doi: 10.1109/ACCESS.2020.2995015.
[16]	O. Evsutin, A. Melman and R. Meshcheryakov, "Digital Steganography and Watermarking for Digital Images: A Review of Current Research Directions," in IEEE Access, vol. 8, pp. 166589-166611, 2020, doi: 10.1109/ACCESS.2020.3022779.
[17]	S. A. Parah et al., "Efficient Security and Authentication for Edge-based Internet of Medical Things," in IEEE Internet of Things Journal, doi: 10.1109/JIOT.2020.3038009.
[18]	B. Hassan, R. Ahmed, B. Li and O. Hassan, "An Imperceptible Medical Image Watermarking Framework for Automated Diagnosis of Retinal Pathologies in an eHealth Arrangement," in IEEE Access, vol. 7, pp. 69758-69775, 2019, doi: 10.1109/ACCESS.2019.2919381.
[19]	G. F. Siddiqui et al., "A Dynamic Three-Bit Image Steganography Algorithm for Medical and e-Healthcare Systems," in IEEE Access, vol. 8, pp. 181893-181903, 2020, doi: 10.1109/ACCESS.2020.3028315.
[20]	X. Cao, Y. Zhou and J. -M. Guo, "Guest Editorial Introduction to Special Section on Modern Reversible Data Hiding and Watermarking," in IEEE Transactions on Circuits

	and Systems for Video Technology, vol. 30, no. 8, pp. 2297-2299, Aug. 2020, doi: 10.1109/TCSVT.2020.3002109.
[21]	X. Yan, Y. Lu, L. Liu and X. Song, "Reversible Image Secret Sharing," in IEEE Transactions on Information Forensics and Security, vol. 15, pp. 3848-3858, 2020, doi: 10.1109/TIFS.2020.3001735.
[22]	P. Eze, U. Parampalli, R. Evans and D. Liu, "A New Evaluation Method for Medical Image Information Hiding Techniques*," 2020 42nd Annual International Conference of the IEEE Engineering in Medicine & Biology Society (EMBC), Montreal, QC, Canada, 2020, pp. 6119-6122, doi: 10.1109/EMBC44109.2020.9176066.
[23]	Zarrabi, H., Emami, A., Khadivi, P. et al. Bless Mark: a blind diagnostically-lossless watermarking framework for medical applications based on deep neural networks. Multimed Tools Appl 79, 22473–22495 (2020). https://doi.org/10.1007/s11042-020-08698-9
[24]	S. Maheshkar, ``Region-based hybrid medical image watermarking for secure telemedicine applications," Multimedia Tools Appl., vol. 76, no. 3, pp. 3617_3647, Feb. 2017.
[25]	R. Thabit and B. E. Khoo, ``Medical image authentication using SLT and IWT schemes," Multimedia Tools Appl., vol. 76, no. 1, pp. 309_332, Jan. 2017.
[26]	B. Lei, E.-L. Tan, S. Chen, D. Ni, T. Wang, and H. Lei, ``Reversible watermarking scheme for medical image based on differential evolution," Expert Syst. Appl., vol. 41, no. 7, pp. 3178_3188, Jun. 2014.
[27]	R. Thabit and B. E. Khoo, ``A new robust lossless data hiding scheme and its application to color medical images," Digit. Signal Process., vol. 38, pp. 77_94, Mar. 2015.